Simulation of the Reduction of Force Ripples of the Permanent Magnet Linear Synchronous Motor

Koon-Seok Chung*, Yu-Wu Zhu*, In-Jae Lee*, Kwon-Soon Lee* and Yun-Hyun Cho†

Abstract - The significant drawback of the permanent magnet linear synchronous motor (PMLSM) is force ripples, which are generated by the distortion of the stator flux linkage distributions, cogging forces caused by the interaction of the permanent magnet and the iron core and the end effects. This will deteriorate the performance of the drive system in high precision applications. The PMLSM and its parasitic effects are analyzed and modeled using the complex state-variable approach. To minimize the force ripple and realize the high precision control, the components of force ripples are extracted first and then compensated by injecting the instantaneous current to counteract the force ripples. And this method of the PMLSM system is realized by the field oriented control method. In order to verify the validity of this proposed method, the system simulations are carried out and the results are analyzed. The effectiveness of the proposed force ripples reduction method can be seen according to the comparison between the compensation and non-compensation cases.

Keywords: Current Injection, Field Oriented Control, Force Ripple, PMLSM

1. Introduction

Linear motor drives are more and more used in factory automation and numerical control systems because they can be operated without indirect coupling mechanisms, such as gear boxes, chains and screw coupling [9], allowing high precision control to be achieved. Permanent magnet linear synchronous motor (PMLSM) drives are probably the most suitable to applications involving high speed and high precision motion control among all types of linear motors. They have certain unique features such as large air-gap, open-wide slots, pole and interpole configurations [8]. The main benefits of PMLSMs include the high force density in the air-gap, a rapid dynamic response, low thermal losses and simple structure.

In spite of such advantages, PMLSM drives may exhibit some drawbacks. A significant and well-known one is the phenomenon of force ripple. The effects of force ripple are particularly undesirable in some demanding motion control and machine tool applications. They lead to speed oscillations, which cause deterioration in the performance [2]. The force ripples change periodically as the mover advances during its motion. The resulting force ripples contain the flux linkage harmonics, cogging harmonics and time harmonics.

Flux linkage harmonics result from the non-sinusoidal flux linkage and from current waveform distortions. And the reluctance torque is very low for permanent magnet machines. In fact, it can be ignored for PMLSMs using the field oriented control method [2]. Cogging force arises from the interaction of the permanent magnets and the ferromagnetic core. This force exists even in the absence of any winding current and it exhibits a periodic relationship with respect to the position of the mover relative to the magnets [6], [8]. Time harmonics are caused by current waveform distortions in the feeding power converter. To minimize their effect, the switching frequency must be high, and the pulse-width modulation scheme must not generate subharmonic currents [11]. This can be satisfied by programming the field control method at 20 [kHz]. The field oriented control algorithm will enable real-time control of force by controlling the q-axis current component. This control structure, by achieving a very accurate steady state and transient control, leads to high dynamic performance in terms of response times and power conversion [5].

In this paper we will extract the force ripples and give explicit function to them. And then only control of the q-axis current can be used to cancel out the force ripples. First, the structure and operating principle of the PMLSMs are described in detail. Second, the space vector modulation is introduced. Thus, appropriate models are then defined for the ripple and a concept for the compensation of force ripple by an adaptive control system is presented, and its effectiveness is demonstrated by some simulation results.

2. Modeling of PMLSM

PMLSMs may be classified into short primary type (long PM poles) and short secondary type (short PM poles) according to their structural features. Fig. 1 shows the basic structure of a short primary type PMLSM. There are alternant N-pole and S-pole permanent magnets fixed on the stator (secondary)

† Corresponding Author: Dept. of Electrical and Electronic Engineering, Dong-A University, Korea (yhcho@dau.ac.kr)
* Dept. of Electrical and Electronic Engineering, Dong-A University, Korea (ywzhu1980@gmail.com)
Received 24 February, 2006 ; Accepted 8 November, 2006

of the PMLSM, and the mover (primary) comprises the armature and windings. The mover will move with the cable, which supplies power by a current-controlled pulse width modulated (PWM) voltage source inverter (VSI) to the PMLSM.

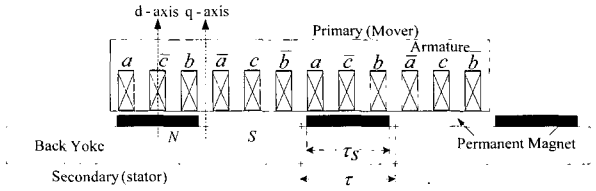

Fig. 1. Structure of PMLSM.

In this paper the space harmonics and force ripple induced by the rotor slots are neglected in a first approach. The following derivation is based on these assumptions: Linear magnetic conditions (no saturation); no temperature or frequency dependence of the resistances and inductances.

Since the flux density field in the air gap is created with permanent magnets attached to the stator, this field will never be perfectly sinusoidal as shown in Fig. 2.

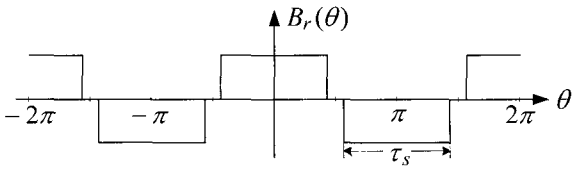

Fig. 2. Flux Density in air-gap.

So the induced flux linkage from the stator magnets in the mover winding can be expressed as a sum of odd cosines where the coefficients decrease rapidly [4]. Thus,

$$\psi_{m,a}(\theta) = \psi_1 \cos\theta + \psi_3 \cos(3\theta) + \psi_5 \cos(5\theta) + \cdots \quad (1)$$

where the amplitude of each flux linkage harmonic depends on the specific design of the stator winding.

We have already known that the PMLSM flux velocity υ_r [1],

$$\upsilon_r = 2\tau_p f_s \quad (2)$$

$$\omega_r = \pi \upsilon_r / \tau_p \quad (3)$$

where υ_r is the electrical velocity, ω_r is the rotating speed, τ_p is pole pitch and f_s is the source frequency.

Based on the upper equations and the fact that the machine is wye-connected with an isolated neutral point, we can derivate the following equations in synchronous rotating reference frame considering the non-sinusoidal components as follows [4]:

$$v_d = R_s i_d + L_d \frac{di_d}{dt} - \frac{\pi}{\tau}\upsilon_r L_q i_q + \frac{\pi}{\tau}\upsilon_r \psi_{d6}\sin(6\theta_r) + \frac{\pi}{\tau}\upsilon_r \psi_{d12}\sin(12\theta_r) + \cdots \quad (4\text{-a})$$

$$v_q = R_s i_q + L_q \frac{di_q}{dt} + \frac{\pi}{\tau}\upsilon_r L_d i_d + \frac{\pi}{\tau}\upsilon_r \psi_m + \frac{\pi}{\tau}\upsilon_r \psi_{q6}\cos(6\theta_r) + \frac{\pi}{\tau}\upsilon_r \psi_{q12}\cos(12\theta_r) + \cdots \quad (4\text{-b})$$

where the equations have been truncated so that they only contain harmonics of up to order 12. Also, $\varphi_m = \varphi_1$ in (4-b). The general expressions for the flux linkage harmonics in (14) are

$$\psi_{dk} = -(k-1)\psi_{k-1} - (k+1)\psi_{k+1} \qquad k = 6,12,\ldots \quad (5\text{-a})$$

$$\psi_{qk} = -(k-1)\psi_{k-1} + (k+1)\psi_{k+1} \qquad k = 6,12,\ldots \quad (5\text{-b})$$

The electromagnetic power can be calculated using the well-known relation

$$P_e = F_x \upsilon_e \quad (6)$$

where υ_e is the mechanical speed of the PMLSM. Since P_e is the electromagnetic power, the force expression becomes [4]

$$F_x(\theta_r) = \frac{3}{2}\cdot n_p \cdot \frac{\pi}{\tau}[\psi_m i_q + (L_d - L_q) i_d i_q + (\psi_{d6}\sin(6\theta_r) + \psi_{d12}\sin(12\theta_r))\cdot i_d + (\psi_{q6}\cos(6\theta_r) + \psi_{q12}\cos(12\theta_r))\cdot i_q] \quad (7)$$

In this force equation, it only considers the harmonics till the 12th, because the higher component of harmonics has very small effects.

And for the surface-mounted PMLSM, the d-axis inductance and q-axis inductance are almost the same, in this paper the field oriented control method is used, which means the d-axis current component i_d is zero, so the thrust can be finally expressed as

$$F_x(\theta_r) = \frac{3}{2}\cdot n_p \cdot \frac{\pi}{\tau}[\psi_m i_q + (\psi_{q6}\cos(6\theta_r) + \psi_{q12}\cos(12\theta_r))\cdot i_q] \quad (8)$$

The difference between the standard model of the PMLSM and the proposed one is that the electrical force of the proposed motor is now a function of the mover position. This leads to force oscillations that have to be minimized in order to control the machine exactly.

In this part we analyzed the model of the PMLSM and gave its mathematics representation only considering the

non-sinusoidal harmonics. A more detailed analysis of harmonics and compensation will be analyzed in the subsequent part.

3. Reduction of Force Ripples

In vector control, a special control is used to make the stator sinusoidal MMF wave quadrature to the permanent magnet fundamental exciting flux, and this is usually called 'field oriented control'. The field oriented control algorithm will enable real-time control of torque and speed. As this control is accurate in every mode of operation (steady state and transient), no oversize of the power transistors is necessary. The transient currents are constantly controlled in amplitude. Moreover, almost no force ripple appears when driving this sinusoidal BEMF motor with sinusoidal current (ideal model).

The basic goal of the control algorithm in this paper is to control the current so that the force ripple is cancelled out. Force variations of very low frequency are normally eliminated by the speed control system. Force harmonics of higher frequency can be compensated in principle by generating an inverse force component through appropriate modulation of the mover current. Because the field oriented control method is used, the modulation of the mover current is in a matter of fact to control the amplitude of q-axis current component i_q.

The design of a permanent magnet motor drive for high performance and minimum force ripple is based on a machine model representing the harmonic effects. So in this paper we first give an appropriate function of force ripples that contains non-sinusoidal flux linkage harmonics and cogging harmonics. Use of the control algorithm compensates these harmonics.

If only considering the ideal model of the PMLSM, the back EMF and force will not contain the harmonics items and (14-a), (14-b) and (21) will be written as:

$$v_d = R_s i_d + L_d \frac{di_d}{dt} - \frac{\pi}{\tau} \upsilon_r L_q i_q \tag{9-a}$$

$$v_q = R_s i_q + L_q \frac{di_q}{dt} + \frac{\pi}{\tau} \upsilon_r L_d i_d + \frac{\pi}{\tau} \upsilon_r \psi_m \tag{9-b}$$

$$F_x = \frac{3}{2} n_p \frac{\pi}{\tau} \psi_m i_q = k_f i_q \tag{10}$$

where $k_f = \frac{3}{2} n_p \frac{\pi}{\tau} \psi_m$.

Not considering the force ripple, the mechanical operating equation can be represented as

$$F_x = M \frac{d\upsilon_r}{dt} + D\upsilon_r + F_l \tag{11}$$

where F_x is the electrical force, M is the total mass of moving element system, D is the viscous friction and iron-loss coefficient, and F_l is the external load force.

Based on (9) ~ (11), the signal flow graph of the PMLSM is visualized in Fig. 3.

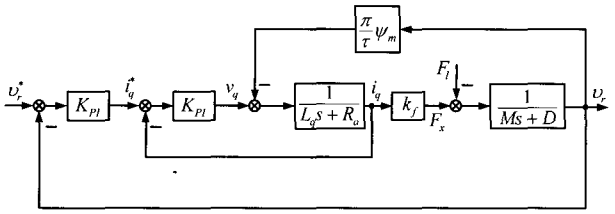

Fig. 3. Control system block diagram.

Fig. 3 shows the adaptive speed control graph of the PMLSM. In the close control loop, the feedback speed υ_r compares with the reference speed value υ_r^*, and then using PI controller adjusts the error between υ_r and υ_r^* to be zero. In this case, it does not consider the harmonics, for high precision and accurate control, we have to analyze and give an appropriate function of harmonics, and then compensate these harmonics.

3.1 Identification of Flux Linkage Harmonics

The effect of flux linkage harmonics is already analyzed and from (8) using the field oriented control method this force harmonics can be seen as

$$F_{x-\psi h}(\theta) = \frac{3}{2} n_p \frac{\pi}{\tau} [\psi_{q6} \cos(6\theta_r) + \psi_{q12} \cos(12\theta_r)] \cdot i_q \tag{12}$$

So the compensated flux linkage force harmonics component force $F_{q-\psi h}$ which is generated by q-axis current component is

$$F_{q-\psi h} = -F_{x-\psi h} \tag{13}$$

This means

$$\frac{3}{2} n_p \frac{\pi}{\tau} \psi_m \cdot i_{q-\psi h} = -\frac{3}{2} n_p \frac{\pi}{\tau} [\psi_{q6} \cos(6\theta_r) + \psi_{q12} \cos(12\theta_r)] \cdot i_q$$

The compensated current $i_{q-\psi h}$ for flux linkage force harmonics is

$$i_{q-\psi h}(\theta_r) = -\frac{\psi_{q6} \cos(6\theta_r) + \psi_{q12} \cos(12\theta_r)}{\psi_m} \cdot i_q \tag{14}$$

Because the flux linkage harmonics current $i_{q-\psi h}$ is far smaller than the reference current i_q, this approximation is sufficiently accurate.

3.2 Identification of Cogging Harmonics

Cogging force comprises two components due to slotting and the finite length of the armature core. It depends on the position of the mover and varies periodically. This cogging harmonic force function $F_{x-ch}(\theta_r)$ is indirectly acquired by operating the machine at very low speed. Because the cogging force is independent of the input current, it is only dependent on the structure of the motor, so the measuring of cogging force is taken in a no-load and low speed case. In this case, from equation (14) it can be seen that the flux linkage harmonics are very small, and the cogging force is predominant. Considering the harmonics, the dynamic equation of the PMLSM can be represented as:

$$F_x = M\frac{dv_r}{dt} + Dv_r + F_l + F_h \tag{15}$$

where F_h is the total harmonics of the PMLSM. It is

$$F_h = F_{x-\psi h} + F_{x-ch} \tag{16}$$

To obtain the cogging harmonics, it has to calculate the total harmonics first.

In the measuring process, because of setting the motor in a no-load operation, F_l is then zero. It keeps the amplitude of input stator current i_q constant, so accordingly (10) the thrust force F_x is constant. Then using the linear encoder to measure the mover position and speed, finally the total harmonics can be calculated by (15)

$$F_h = F_x - M\frac{dv_r}{dt} - Dv_r \tag{17}$$

In the test, its ac content is the force ripple, and the dc offset is the load force including friction of the motor. After getting the total force ripple, just minus the flux linkage force ripple, the cogging harmonics is obtained, and then the corresponding compensating q-axis current component is

$$i_{q-ch}(\theta_r) = \frac{F_h - F_{x-\psi h}}{k_f} \tag{18}$$

For the upper analysis, both flux linkage and cogging force harmonics vary with the mover position θ_r. Using the field oriented control method the control diagram can be drawn as in Fig. 4. The shaded part is the compensation part.

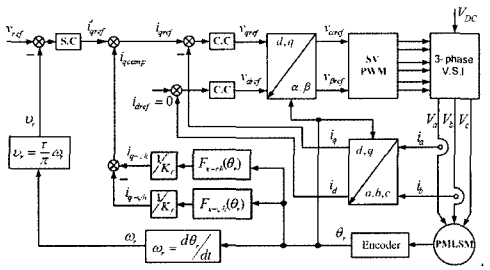

Fig. 4. Control diagram of PMLSM.

In the control diagram of a PMLSM, first it samples the phase currents i_a and i_b, then it transfers them into rotor-fixed frame components i_d and i_q by Clarke and Park transformation. Secondly, according to the reference speed and the sampled mover speed of the PMLSM to calculate the q-axis current component i'_{Sqref} by PI (Proportional-Integral) speed controller and considering the harmonics, the reference current i_{qref} is the sum of i'_{qref} and i_{qcomp}, . Because the field oriented control algorithm is used, the d-axis reference current is $i_{dref} = 0$. Thirdly, PI current controllers are used to calculate d-axis reference voltage v_{dref} and q-axis reference voltage v_{qref} in terms of the errors between i_{qref} and i_q , i_{dref} and i_d respectively. Finally the Park-1 transformation is used to to obtain $v_{S\alpha ref}$, and $v_{S\beta ref}$ and to modulate the space vector PWM to offer the motor suitable voltage to maintain the constant speed of the PMLSM.

Table 1. Specification of PMLSM.

Parameter	Value	Parameter	Value
Rotor magnet material	NeFeB	LSM width	52.8 mm
Rated voltage (DC)	50 V	Pole pitch	30 mm
Rated current	5 A	Magnetic pole pitch	25 mm
Rated force	160N	Air-gap length	2 mm
Rated velocity	1.2 m/s	Slot numbers	12
Winding turns per pole per phase	40 turns	Slot numbers per pole per phase	1
Number of pole pairs	2	Armature resistance	0.75 Ω
Mover mass	2.0 Kg	d-axis inductance	0.85mH
Fundamental flux linkage	103.9 mWb	q-axis inductance	0.85 mH

4. Simulated Results

The specifications of the PMLSM are shown in Table I.

Since we have known the parameters, we can first simulate the performance of the PMLSM and obtain some

results in theory.

In this paper, the PI current controllers and the PI speed controller parameters are:

$$K_{pd} = K_{pq} = 4$$
$$K_{id} = K_{iq} = 400$$
$$K_{pv} = 0.15$$
$$K_{iv} = 6.0$$

The simulation is realized by the C++ language program and the results are shown in Matlab. This simulation contains the rated speed 1.2 [m/s] command responses, speed switch responses and the load switch responses. In the simulation, the comparisons between the non-compensated ripple and compensated ripple are taken, and it can be seen that the results of the compensation are very effective.

4.1 Rated Speed 1.2 [m/s] Command Responses

In this case, the motor was taken into rated speed 1.2 [m/s] command from standstill without load. We observed the phase current, speed, and force, respectively.

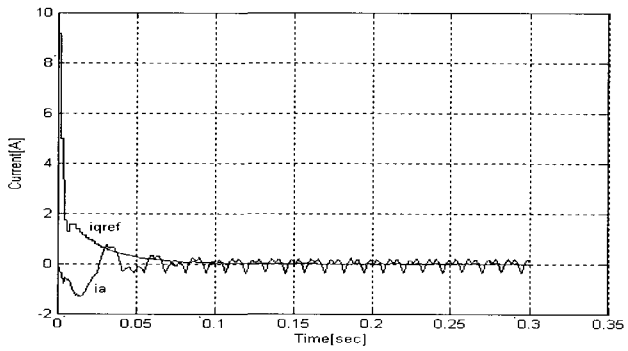

(a)

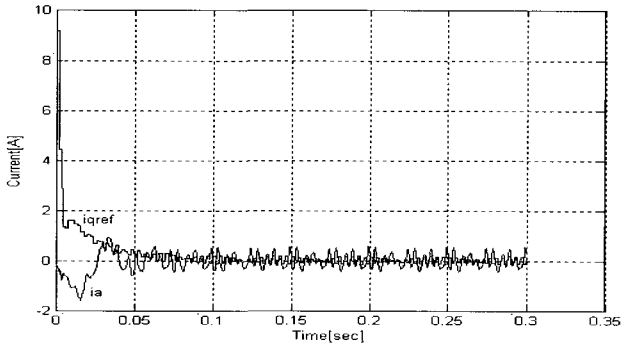

(b)

Fig. 5. Current Waveform of PMLSM. (a) No compensation; (b) Compensation.

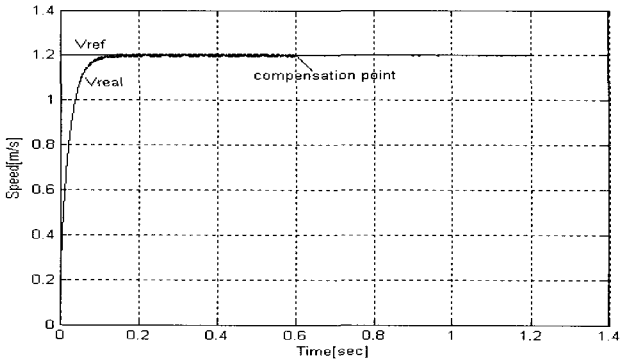

(a)

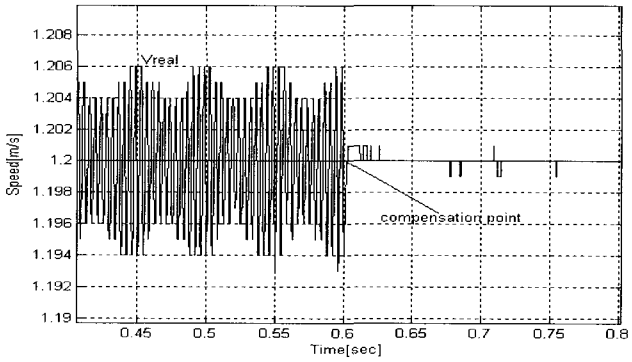

(b)

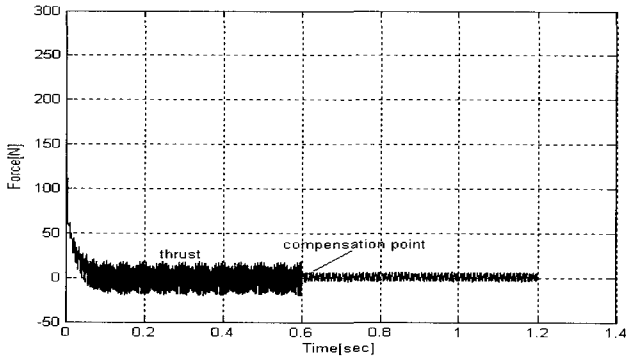

(c)

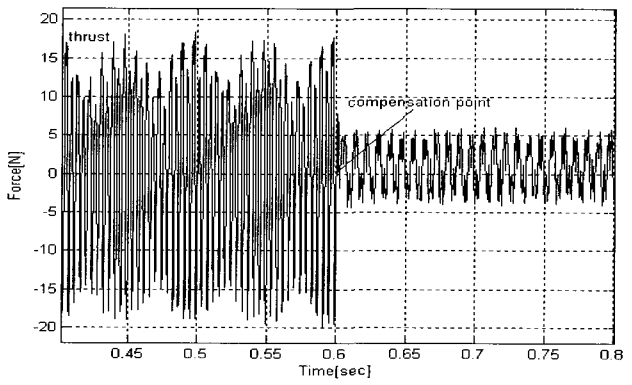

(d)

Fig. 6. Waveforms under Rated Speed Command. (a) Speed; (b) Speed blow-up; (c) Force; (d) Force blow-up.

It can be seen that the current in Fig. 5(b) has a much higher component than that in Fig. 5(a), which is the injected current to counteract the force ripple. The corresponding speed and force responses can be seen in Fig. 6. It takes the compensation command at 0.6 [sec], and Figs. 6 (b) and (d) are the enlargements of Figs. 6 (a) and (c) around the compensation point. It can be seen that the speed and force ripples are significantly suppressed.

4.2 Reference Speed Switch Command Responses

In this section the speed command is given at 0.8 [m/s] and keeps to 0.4 [s] at the beginning, after which it changes into the rated speed command 1.2 [m/s] and also keeps 0.4 [s]. At this point, it finally changes into 0.8 [m/s] again. We can see the responses waveform in Fig. 7. There is a significant force to make the mover achieve the command speed when the speed command changes, and the force ripples are reduced under any speed command.

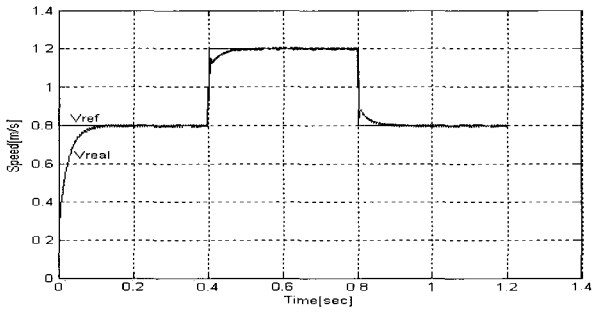

(a)

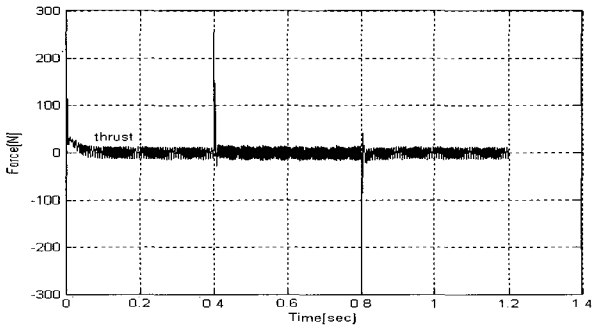

(b)

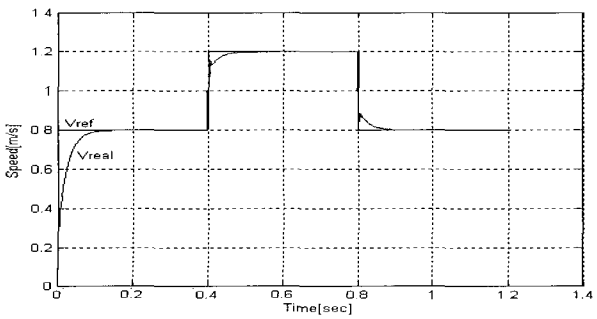

(c)

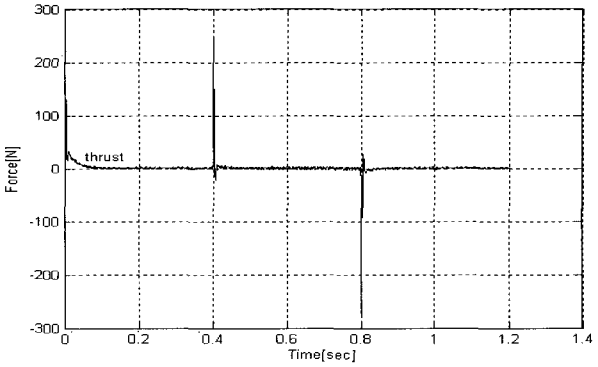

(d)

Fig. 7. Waveforms under different speed commands. (a) Speed no-compensation; (b) Force no-compensation; (c) Speed compensation; (d) Force compensation.

4.3 Load Switch Command Responses

Fig. 8 shows the responses under the condition that the PMLSM operates at rated speed 1.2 [m/s] and adds the 1/2 rated load 80 [N] during the period from 0.4 [s] to 0.8 [s]. In the comparison it can be seen that the ripples are minimized. Especially in the no load case, the force ripple is significantly reduced and the compensation is very effective to smooth this ripple. For adding the load case, although the force ripple is obvious after compensation, it is ignorable to the load because there is almost no effect to speed.

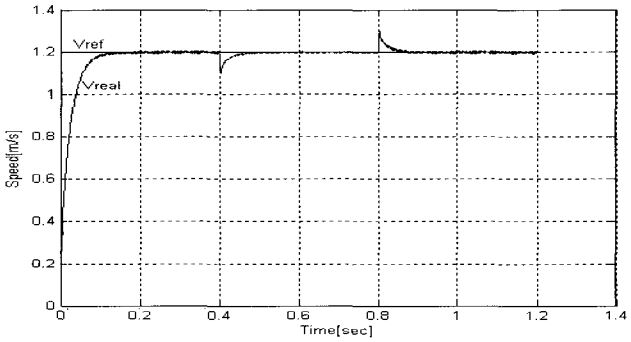

(a)

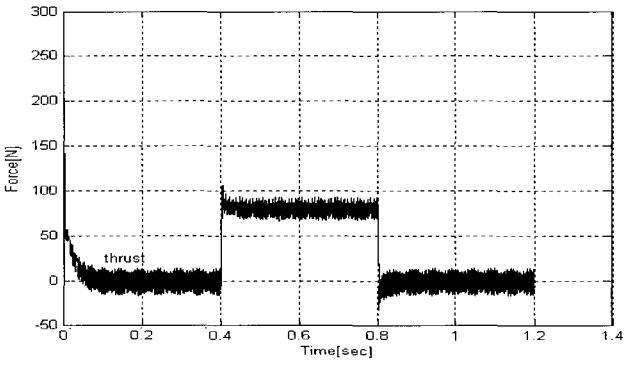

(b)

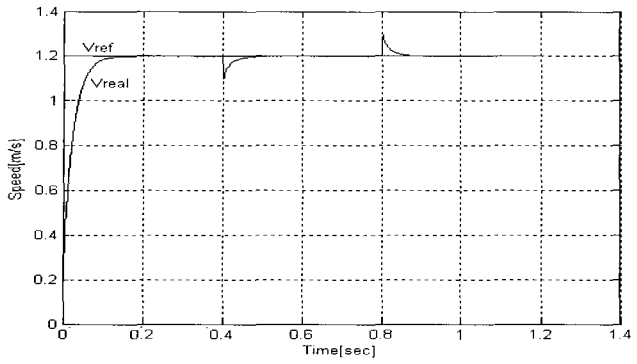

(c)

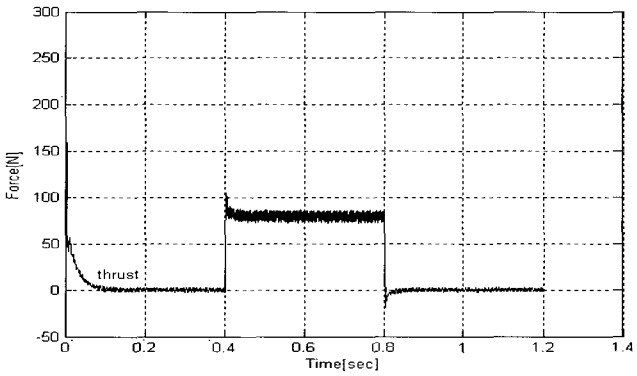

(d)

Fig. 8. Waveforms under No-Load and Load Commands. (a) Speed no-compensation; (b) Force no-compensation; (c) Speed compensation; (d) Force compensation.

According to the above simulation results, it proves this force ripple compensation method is effective under any case.

5. Conclusion

In this paper we first give an appropriate function of force ripples which contain non-sinusoidal flux linkage harmonics and cogging harmonics. It is feasible to implement the compensation for the explicit function easily using the field oriented control method. The simulation results, under different speed and load conditions, verified that the proposed algorithm is very effective.

Acknowledgments

This research was supported by the Program for the Training of Graduate Students in Regional Innovation which was conducted by the Ministry of Commerce Industry and Energy of the Korean Government.

References

[1] FAA-JENG LIN, KUO-KAI SHYU, and CHIH-HONG LIN, "Incremental Motion Control of Linear Synchronous Motor", *IEEE. Trans. on Aerospace and Electronic System*, vol. 38. No. 3, July 2002.

[2] Joachim Holtz, "Identification and Compensation of Torque Ripple in High-Precision Permanent Magnet Motor Drives", *IEEE. Trans. on Industrial Electronics*, vol. 43. No. 2, April 1996.

[3] B.-J. Brunsbach, G. Henneberger, and Th. Klepsch, "Compesation of Torque Ripple", *University of Technology Aachen, Germany*, pp. 588-593.

[4] Oskar Wallmark, "Modelling of Permanent-Magnet Synchronous Motors Machines with Non-Sinusoidal Flux Linkage", Chalmers University of Technology, Sweden.

[5] "Field Oriented Control of 3-Phase AC-Motor", Texas Instruments Europe, February 1998.

[6] K.K. Tan, S.N. Huang, and T.H. Lee "Robust Adaptive Numerical Compensation for Friction and Force Ripple in Permanent-Magnet Linear Motor", *IEEE. Trans. on Magnetics*, vol. 38. No. 1, January 2002.

[7] Nicola Bianchi, Silverio Bolognani, and Alessandro Dalla Francesca Cappello, "Back E.M.F Improvement and Force Ripple Reduction in PM Linear Motor Drives", *35th Annual IEEE Power Electronics Specialiists Conference. Achen, Germany*, 2004.

[8] P.J. Hor, Z.Q. Zhu, D. Howe, J. Rees-Jones, "Minimization of Cogging Force in a Linear Permanent Magnet Motor", *IEEE Trans. on Magnetics*, vol. 34, No. 5, September 1998.

[9] K.K. Tan, S. Zhao, "Adaptive Force Ripple Suppression in Iron-core Permanent Magnet Linear Motors", *Proceeding of the 2002 IEEE International Symposium on Intelligent Control, Vancouver, Canada*, October, 2002.

[10] N. Bodika, R.J. Cruise, and C.F. Landy, "Design of a PI Controller to Counteract the Effect of Cogging Forces in a Permanent Magnet Synchronous Linear Motor", *IEEE, University of the Wiwatersrand, Johannesburg, South Africa*, 1999.

[11] J. Holtz, "pulsewidth modulation—A Survey", IEEE Trans. Ind. Electron, vol. 39, No. 5, pp. 410-420, October 1992.

Koon-Seok Chung
He is a graduate student in the Doctor's program at Dong-A University. He received his Master's degree from Dong-A University in 1997. His research interests are in the area of motor design and control.

Yu-Wu Zhu
He is a graduate student in the Doctor's program at Dong-A University. He received his Master's degree from Dong-A University in 2005. His research interests are in the area of linear motor control, DSP and control systems.

In-Jae Lee
He is a graduate student in the Master's program at Dong-A University. He received his Bachelor's degree from Dong-A University in 2005. His research interests are in the area of motor control and drivers.

Kwon-Soon Lee
He is a Professor at Dong-A University. He received his Master's degree from Seoul University in 1981, and his D. degree from Oregon State University in 1990. His research interest is in control methods.

Yun-Hyun Cho
He is a Professor at Dong-A University. He received his Master's degree from Hanyang University in 1986, and his D. degree from Hanyang University in 1991. His research interests are in the fields of power, electric drives and control system.